

Learning to Predict Gradients for Semi-Supervised Continual Learning

Yan Luo, Yongkang Wong, *Member, IEEE*, Mohan Kankanhalli, *Fellow, IEEE*, and Qi Zhao, *Member, IEEE*

Abstract—A key challenge for machine intelligence is to learn new visual concepts without forgetting the previously acquired knowledge. Continual learning is aimed towards addressing this challenge. However, there is a gap between existing supervised continual learning and human-like intelligence, where human is able to learn from both labeled and unlabeled data. How unlabeled data affects learning and catastrophic forgetting in the continual learning process remains unknown. To explore these issues, we formulate a new semi-supervised continual learning method, which can be generically applied to existing continual learning models. Specifically, a novel gradient learner learns from labeled data to predict gradients on unlabeled data. Hence, the unlabeled data could fit into the supervised continual learning method. Different from conventional semi-supervised settings, we do not hypothesize that the underlying classes, which are associated to the unlabeled data, are known to the learning process. In other words, the unlabeled data could be very distinct from the labeled data. We evaluate the proposed method on mainstream continual learning, adversarial continual learning, and semi-supervised learning tasks. The proposed method achieves state-of-the-art performance on classification accuracy and backward transfer in the continual learning setting while achieving desired performance on classification accuracy in the semi-supervised learning setting. This implies that the unlabeled images can enhance the generalizability of continual learning models on the predictive ability on unseen data and significantly alleviate catastrophic forgetting. The code is available at https://github.com/luoyan407/grad_prediction.git.

Index Terms—Continual learning, semi-supervised learning, gradient prediction.

1 INTRODUCTION

CONTINUAL learning models continuously observe sets of labeled data through a sequence of tasks [1], [2]. The tasks may vary over time, *e.g.* images with novel visual concepts (*i.e.* classes) or addressing different problems from the previous tasks [3]. Continual learning is analogous to human-like learning. Humans are able to continually acquire, adjust, and transfer knowledge and experiences throughout their lifespan. The key challenges are two-fold. First, the learning models can abruptly forget previously absorbed knowledge while learning new information in novel tasks, *i.e.* suffer from catastrophic forgetting [4]. Second, how to leverage the knowledge learned from previous tasks to quickly adapt to novel tasks.

The fundamental challenge lies in the generalizability of learning over various tasks. As most of the modern continual learning methods are gradient-based [5], [6], [7], [8], [9], [10], [11], [12], [13], [14], the model is learned through model update with gradients computed from the data and the corresponding ground-truth. In other words, the information of the labeled data is transferred and extracted to form the knowledge acquired by the model through gradient descent.

A straightforward yet effective way to enhance the generalizability is to use more labeled data for training [15]. Unfortunately, large-scale labeled data may not always be available because collecting high quality human annotations is labor-intensive. Therefore, incorporating unlabeled data

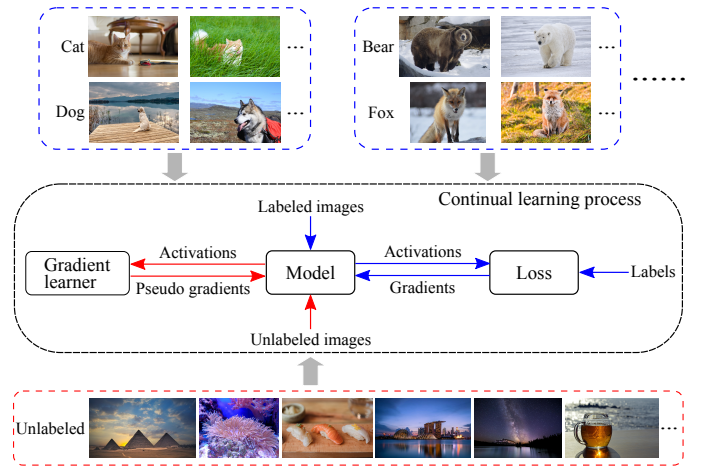


Figure 1: Problem of semi-supervised continual learning. Conventional supervised continual learning requires labels to compute gradients for model update (see blue flows). In contrast, this work proposes to *predict gradients* so that the unlabeled images can be leveraged into the continual learning paradigm for better generalizability (see red flows).

with the labeled data for training is a feasible and common approach. Pseudo labeling, *i.e.* generating artificial labels by a teacher network for the unlabeled data and taking them as the ground-truth labels for training a student network, is widely used for semi-supervised learning (SSL) [16], [17], [18], [19]. However, it may not work in semi-supervised continual learning (SSCL) where the classes of a task are distinct from the ones in the other tasks or the task's labels may be of a different form, *e.g.* category vs. bounding box. In addition,

- Y. Luo and Q. Zhao are with the Department of Computer Science and Engineering, University of Minnesota, Minneapolis, MN, 55455. E-mail: luoxx648@umn.edu & qzhao@cs.umn.edu
- Y. Wong and M. Kankanhalli are with the School of Computing, National University of Singapore, Singapore, 117417. E-mail: yongkang.wong@nus.edu.sg & mohan@comp.nus.edu.sg

Manuscript received April XX, 2021; revised July XX, 202X.

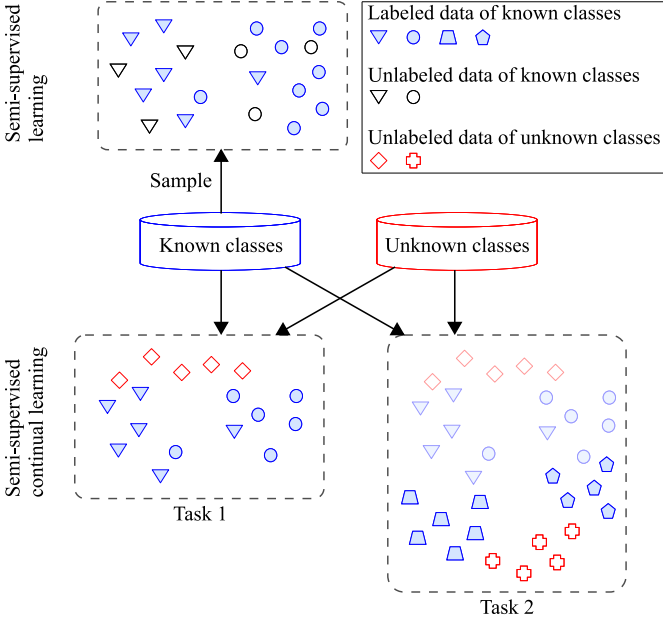


Figure 2: Conceptual comparison between the challenge in the novel *semi-supervised continual learning* (SSCL) problem and the one in the *semi-supervised learning* (SSL) problem. The key difference is that the underlying classes w.r.t. the unlabeled data could be unknown in the SSCL problem, while the ones in SSL are assumed to be from the known classes. To amenably adapt to the continual learning paradigm, we do not impose such a hypothesis in the novel SSCL problem. Instead, the underlying labels of unlabeled data can be from either known classes or unknown classes. The fade-out samples in the task 2 indicate that the samples in the task 1 are not available in the task 2 according to the protocol.

pseudo labeling methods assume that the unlabeled data share similar class labels with the labeled data. We do not make such an assumption. Instead, the unlabeled data could have either the same or different class labels as the labeled data, which is shown in Fig. 2. In contrast to pseudo labeling methods, learning to predict pseudo gradients on unlabeled samples is straightforward and effective as predicting labels is skipped. Moreover, the pseudo gradients are aligned with the knowledge learned from samples in various categories, while the gradients generated by pseudo labeling methods are aligned with a specific category as an unlabeled sample is conventionally labeled as a category in the continual learning setting.

To utilize unlabeled data into the supervised continual learning framework, we propose a novel gradient-based learning method that learns from the labeled data to predict *pseudo gradients* for the unlabeled data, as shown in Fig. 1. Specifically, a novel gradient learner learns the mapping between features and the corresponding gradients generated with labels. We follow [7], [8] to conduct comprehensive experiment on continual learning benchmarks, *i.e.* MNIST-R, MNIST-P, iCIFAR-100, CIFAR-100, and miniImageNet. To verify the generalization ability of the proposed method, we follow [20] to evaluate the proposed method on SVHN, CIFAR-10, and CIFAR-100. The main contributions of this

work are recapped as follows.

- We propose a novel semi-supervised continual learning (SSCL) method that leverages the rich information from unlabeled data to improve the generalizability of continual learning models.
- We propose a learning method that learns to predict gradients for unlabeled data. To the best of our knowledge, this is the first work that generates pseudo gradients without ground-truth labels.
- Extensive experiments and ablation study show that the proposed method improves the generalization performance on all metrics, namely average accuracy, backward transfer, and forward transfer. This implies that learning with unlabeled data is helpful for improving the predictive ability of continual learning models and for alleviating catastrophic forgetting.
- We provide empirical evidence to show that the proposed method can generalize to the SSL task.

2 RELATED WORK

2.1 Continual Learning

Continual learning problem is defined as a process of learning through a sequence of tasks [1], [2], [21], which is a branch of online learning [22], [23], [24]. The challenge in this learning paradigm is to achieve a desired trade-off between retaining knowledge about preceding tasks and acquiring new information for future tasks. Catastrophic forgetting is prone to occur in this learning paradigm [4]. There are a number of works that study this problem [5], [6], [7], [8], [9], [10], [11], [12], [13], [14], [25], [26], [27], [28], [29], [30]. Specifically, Lopez-Paz and Ranzato propose a memory-based method, namely GEM, to impose a constraint on the gradients w.r.t to the training samples and the memory [8]. Along the same line, Luo *et al.* introduce a gradient alignment method DCL that enhances the correlation between the gradient and the accumulated gradient [9]. Recently, Ebrahimi *et al.* propose an adversarial continual learning (ACL) approach that aims to factorize task-specific and task-invariant features simultaneously [7]. Unlike GEM, where the training samples are observed one by one, the training process of ACL would repeat multiple times on every task. All the aforementioned works follow supervised continual learning paradigm that requires the ground-truth labels. However, how unlabeled data may influence the continual learning problem remain unclear. In this work, we propose the SSCL paradigm, where the model observes unlabeled data sometimes.

2.2 Class-incremental Learning

This learning problem aims to learn visual concepts in new tasks while retaining the visual concepts learned in the previous tasks [26], [31], [32]. Correspondingly, the samples in the coresets would be repeatedly observed in this problem, whereas continual learning only observes each sample once. Lee *et al.* study how to leverage unlabeled data with a knowledge distillation method to boost the class-incremental learning [31]. Specifically, the experimental protocol in [31] is different from that of the SSCL. The class-incremental learning with unlabeled data maintains three

sets of samples through the learning process, *i.e.* the samples that have been seen in the previous tasks, the samples that are related to the current task and have not been seen before, and the unlabeled samples are selected by a confidence-based strategy from a data pool. In contrast, the SSCL only observes the samples that are related to the current task and the unlabeled samples randomly selected from the data pool. For a fair comparison, we utilize the knowledge distillation method that is used in [31] to generate pseudo labels for unlabeled samples as the baselines.

2.3 Semi-supervised Learning (SSL)

Existing methods are mainly based on pseudo-labeling or self-training, *i.e.* leveraging the labeled data to predict artificial labels for the unlabeled data [33], [34]. Most modern deep learning based models follow this line of research [16], [17], [19], [20], [35], [36], [37], [38], [39], [40], [41]. Particularly, the noisy student model [19] employs the teacher-student method to train on ImageNet [15] with unlabeled images from JFT [42] to achieve state-of-the-art performance. In addition, Zhang *et al.* propose a meta-objective to alternately optimize the weights and the pseudo labels such that the learning process can leverage unlabeled data [20]. Different from conventional (semi-)supervised learning, where visual concepts are unchanging during the learning process, the visual concepts of a task in continual learning are different from that of the other tasks through the whole learning process. As a result, unlabeled data that are labeled as known classes would break the protocol of the split of classes in various tasks of continual learning [8]. Instead, the continual learning is in favor of a more generic hypothesis of unlabeled data, that is, the underlying labels of unlabeled data could be unknown. A natural choice is to sample unlabeled images from external datasets, rather than treating training images as unlabeled images.

2.4 Gradient-based Methods

Gradient is an essential element for updating the model in deep learning [8], [9], [39], [43], [44], [45], [46]. In supervised learning, the learning process is composed by the forward propagation and back-propagation. Jaderberg *et al.* propose a learning framework with the synthetic gradients to allow layers to be updated in an asynchronously fashion [47]. The proposed pseudo gradients can be used as ground-truth gradients in such a learning framework when the labels of training images are missing. In particular, [8], [9] use the information of gradients to form a constraint to improve continual learning. [43], [44], [46] have a similar flavor, that is, they aim to learn an optimizer to adaptively compute the step length for the vanilla gradients. In contrast with previous gradient-based works, to the best of our knowledge, this is the first work that studies how to generate gradients for the unlabeled images of unknown classes in the continual learning setting.

Stochastic optimization methods often use gradients to update a model's parameters. In the literature, stochastic gradient descent (SGD) [48] takes the anti-gradient as the parameters' update for the descent, using the first-order approximation [49]. In a similar manner, several first-

and second-order methods are devised to guarantee convergence to local minima under certain conditions [50], [51], [52]. Nevertheless, these methods are computationally expensive and may be not feasible for learning settings with large-scale high-dimensional data. In contrast, adaptive methods, such as Adam [53], RMSProp [54], and Adabound [55], show remarkable efficacy in a broad range of machine learning tasks [53], [54], [55]. Moreover, Zhang *et al.* propose an optimization method that wraps an arbitrary optimization method as a component to improve the learning stability [56]. These methods are contingent on vanilla gradients to update a model. In this work, we study how the predicted gradients influence the learning process.

3 PROBLEM SET-UP

The training process of supervised learning methods generally requires a training dataset $D_{tr} = \{(x_i, y_i)\}_{i=1}^I$ that consists of samples $s_i = (x_i, y_i)$, where $x_i \in \mathcal{X}$ represents a feature vector and $y_i \in \mathcal{Y}$ represents a target vector, where \mathcal{Y} is the target label space. The samples presumably are identically and independently distributed variables that follow a fixed underlying distribution \mathcal{D} [8]. With all samples, supervised learning methods attempt to find a model $f : \mathcal{X} \xrightarrow{\theta} \mathcal{Y}$ to map feature vectors to the target vectors, where θ are the parameters of f . In contrast to supervised learning, supervised continual learning is more human-like and will observe the continuum of data

$$D_{tr} = \{(x_i, t_i, y_i) | (x_i, y_i) \sim \mathcal{D}_{t_i}, t_i \in \mathcal{T}\},$$

where t_i indicates the i -th task and \mathcal{T} is a set of tasks. A task is a specific learning problem. Different from supervised learning, which has a fixed distribution, each task is associated with an underlying distribution in the supervised continual learning setting. The supervised continual learning models are defined as $f : \mathcal{X} \times \mathcal{T} \xrightarrow{\theta} \mathcal{Y}$. Correspondingly, the loss of supervised continual learning is defined as

$$\mathcal{L}(f_{\theta}, D_{tr}) = \frac{1}{|D_{tr}|} \sum_{(x_i, t_i, y_i) \in D_{tr}} \ell(f_{\theta}(x_i, t_i), y_i), \quad (1)$$

where $f(\cdot; \theta)$ is simplified as $f_{\theta}(\cdot)$. With the loss function ℓ and a training sample (x_i, t_i, y_i) , the gradient can be computed, *i.e.* $\frac{\partial \ell}{\partial z_i} \frac{\partial z_i}{\partial \theta}$, where $z_i = f_{\theta}(x_i, t_i)$. Typically, ℓ is the cross entropy loss in the classification task. Note that we follow the convention of classification literature [57], [58], [59] to define the input of ℓ as logits z and ground-truth labels y , instead of predicted labels and ground-truth labels. Finally, the model is updated with the computed gradient, that is,

$$\theta \leftarrow \theta - \eta \frac{\partial \ell}{\partial z_i} \frac{\partial z_i}{\partial \theta}, \quad (2)$$

where η is the learning rate for updating θ .

In this work, we define semi-supervised continual learning (SSCL) as the process that continual learning models learn from both labeled data and unlabeled data. If the input is the unlabeled data $\tilde{x}_i \in \tilde{\mathcal{X}}$, the model update (2) is not applicable. Therefore, the key problem in this work is to study how to generate a pseudo gradient g for updating

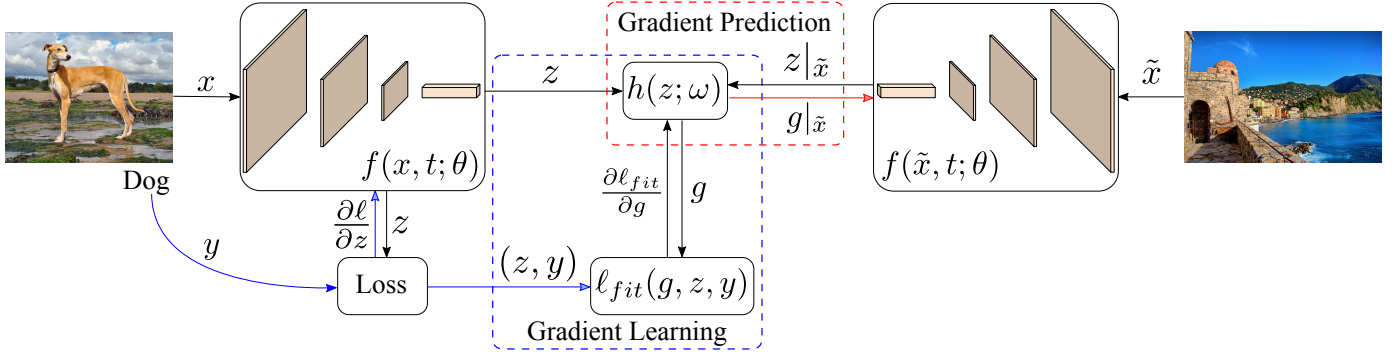


Figure 3: Overview of the proposed gradient learning and gradient prediction process with the gradient learner $h(\cdot; \omega)$. The backbone network is shared between the two processes.

the model. Correspondingly, the model update (2) would be changed to

$$\theta \leftarrow \theta - \eta g|_{\tilde{x}_i} \frac{\partial g|_{\tilde{x}_i}}{\partial \theta}. \quad (3)$$

where $g|_{\tilde{x}_i}$ indicates that the pseudo gradient g is computed with the unlabeled data \tilde{x}_i . Moreover, we aim to study how \tilde{X} influences the learning process of continual learning [8] and adversarial continual learning [7].

4 METHODOLOGY

In this section, we introduce how to train a gradient learner in a continual learning framework, and how to use the resulting gradient learner to predict gradients of unlabeled data. We also discuss the sampling policy for unlabeled data and the geometric interpretation of the proposed gradient prediction. Fig. 3 shows an overview of the proposed SSCL method, which includes *gradient learning* and *gradient prediction* process.

4.1 Gradient Learning

In a continual learning framework, a model is designed to learn the mapping from raw data to the logits that minimize the pre-defined continual loss. During the training process, at the i -th training step or episode, the generated logits z_i w.r.t. the input x_i is passed to the continual loss ℓ . With the corresponding y_i , $\ell(z_i, y_i)$ is computed to yield the gradient $\frac{\partial \ell}{\partial z_i}$. We aim to compute the pseudo gradient \bar{g} and use it to back-propagate the error and update the parameters θ by the chain rule. They can be mathematically summarized as

$$\text{Forward: } z_i = f_\theta(x_i, t_i), \quad (4)$$

$$\text{Backward: } \frac{\partial \ell}{\partial \theta} = \frac{\partial \ell}{\partial z_i} \frac{\partial z_i}{\partial \theta}, \quad \theta \leftarrow \theta - \eta \frac{\partial \ell_{fit}}{\partial \bar{g}} \frac{\partial \bar{g}_i}{\partial \omega}. \quad (5)$$

When the learning process is fed with unlabeled data \tilde{x}_i , it is desirable to have the logits and corresponding gradient so that \tilde{x}_i can straightforwardly fit into the supervised continual learning framework. Therefore, we propose a gradient learner h that aims to learn the mapping from the logits z_i to the gradients $\frac{\partial \ell}{\partial z_i}$, that is,

$$g_i = h(z_i; \omega), \quad (6)$$

where ω is the parameters of h and g_i is the predicted gradient that is expected to work as $\frac{\partial \ell}{\partial z_i}$ for back-propagation.

To guarantee that the predicted gradients can mimic the gradients' efficacy in the learning process, we formulate the fitness of the predicted gradients w.r.t. the logits as a learning problem. We define the fitness loss to quantify the effect of the predicted gradients by fitting them back in the loss, *i.e.*

$$\ell_{fit}(z_i, g_i, y_i) = \ell(z_i - \eta g_i, y_i). \quad (7)$$

By observing triplet (z_i, g_i, y_i) at each training step, the minimization of ℓ_{fit} will iteratively update the proposed gradient learner $h(\cdot; \omega)$ through back-propagation. As depicted in Eq. (7), the predicted gradients aim to minimize the fitness loss, rather than mimicking the vanilla gradients $\frac{\partial \ell}{\partial z}$ in terms of direction and magnitude.

However, the gradients are sensitive in the learning process and a small change in gradients could lead to a divergence of training. To obtain robust predicted gradients, instead of directly using the output of $h(\cdot; \omega)$ in the fitness loss (7), we reference the magnitude τ_i of the vanilla gradient. With τ_i , the predicted gradient can be accordingly normalized, *i.e.*

$$\bar{g}_i = \alpha \tau_i g_i / \|g_i\|, \quad \tau_i = \left\| \frac{\partial \ell}{\partial z_i} \right\|, \quad (8)$$

where $\alpha \in [0, 1]$ is a hyperparameter that controls the proportion of the magnitude of the predicted gradient to τ_i and z_i is generated by (x_i, t_i, y_i) . On the other hand, the output of the proposed gradient learner is a gradient that is subtle and crucial to the learning process. To properly update the proposed gradient learner, we apply a simple yet practically useful version of the loss scale technique [60], [61], [62] to the fitness function. Specifically, the left hand side in Eq. (7) is multiplied with a pre-defined coefficient λ . Finally, the fitness loss is computed with more robust \bar{g}_i , that is

$$\ell_{fit}(z_i, \bar{g}_i, y_i) = \lambda \ell(z_i - \eta \bar{g}_i, y_i). \quad (9)$$

Once the fitness loss is set, triplet (z, \bar{g}, y) at each training step suffices to fit into the model learning. Specifically, the proposed gradient learner would be updated with $\frac{\partial \ell_{fit}}{\partial \bar{g}_i}$, *i.e.*

$$\omega \leftarrow \omega - \hat{\eta} \frac{\partial \ell_{fit}}{\partial \bar{g}_i} \frac{\partial \bar{g}_i}{\partial \omega}. \quad (10)$$

where $\hat{\eta}$ is the learning rate for updating ω . The model learning formed by the fitness loss (7) and the update

Algorithm 1 Gradient Learning & Prediction

```

1: Input:  $(x_i, t_i, y_i) \in D_{tr}, \tilde{x}_i, \theta, \omega, \alpha, \lambda, \eta, \hat{\eta}$ 
2:  $z_i = f(x_i, t_i; \theta)$ 
3:  $\ell_i = \ell(z_i, y_i)$ 
4: Compute the gradient w.r.t.  $z_i$ , i.e.  $\frac{\partial \ell_i}{\partial z_i}$ 
5: Update the model  $\theta \leftarrow \theta - \eta \frac{\partial \ell_i}{\partial z_i} \frac{\partial z_i}{\partial \theta}$ 
6:  $g_i = h(z_i; \omega)$ 
7:  $\bar{g}_i = \alpha \tau_i g_i / \|g_i\|, \quad \tau_i = \|\frac{\partial \ell_i}{\partial z_i}\|$ 
8:  $\ell_{fit} = \lambda \ell(z_i - \eta \bar{g}, y_i)$ 
9: Compute the gradient w.r.t.  $\bar{g}_i$ , i.e.  $\frac{\partial \ell_{fit}}{\partial \bar{g}_i}$ 
10: Update the gradient learner  $\omega \leftarrow \omega - \hat{\eta} \frac{\partial \ell_{fit}}{\partial \bar{g}_i} \frac{\partial \bar{g}_i}{\partial \omega}$ 
11: if  $\tilde{x}_i$  is not equal to  $\emptyset$  then
12:    $z|_{\tilde{x}_i} = f(\tilde{x}_i, t_i; \theta), \quad g|_{\tilde{x}_i} = h(z|_{\tilde{x}_i}; \omega)$ 
13:    $\bar{g}|_{\tilde{x}_i} = \alpha \tau_i g|_{\tilde{x}_i} / \|g|_{\tilde{x}_i}\|, \quad \tau_i = \|\frac{\partial \ell}{\partial z_i}\|$ 
14:    $\theta \leftarrow \theta - \eta \bar{g}|_{\tilde{x}_i} \frac{\partial \bar{g}|_{\tilde{x}_i}}{\partial \theta}$ 
15: end if

```

function (10) is generic and any gradient-based methods, e.g. multilayer perceptron (MLP) [63], deep networks [57], [58], [59], or transformer [64], can be used. Without loss of generality, we use the baseline gradient-based method, i.e. MLP, in this work.

The process of learning to predict pseudo gradients is described in lines 6–10 in Algorithm 1.

4.2 Gradient Prediction

To avail the additional unlabeled data in the learning process for better generalizability, the proposed gradient learner h will predict gradients when the learning process is fed with unlabeled data \tilde{x} . Given \tilde{x}_i , the predicted gradient is computed in a similar way as Eq. (6) and (8) describe, but we use $\tau_{i-1} = \|\frac{\partial \ell}{\partial z_{i-1}}\|$ (i.e. the last labeled sample prior to the n -th step), rather than τ_i , as the label of \tilde{x}_i is absent to produce $\|\frac{\partial \ell}{\partial z_i}\|$. Once the predicted gradient $\bar{g}|_{\tilde{x}_i}$ is computed, the model can be updated as

$$\theta \leftarrow \theta - \eta \bar{g}|_{\tilde{x}_i} \frac{\partial \bar{g}|_{\tilde{x}_i}}{\partial \theta}. \quad (11)$$

To maintain the flexibility in leveraging external unlabeled data, we follow the basic idea of probability theory to presume that unlabeled data are sampled from a distribution. In contrast with the use of labeled data, where we assume all labeled data will be used during the training process, it is possible that no unlabeled data are sampled at some learning steps. In other words, the training process will revert to supervised learning if no unlabeled data is used. Mathematically, it can be formulated as

$$\tilde{x} = \begin{cases} \tilde{x}_i \sim \mathcal{D}_{\tilde{x}}, & \text{if } q < p \\ \emptyset, & \text{otherwise} \end{cases} \quad (12)$$

where q is a random variable following a distribution and p is a pre-defined threshold. Without loss of generality, we assume the distribution is a standard uniform distribution $\mathcal{U}(0, 1)$. When p is set to 1, it indicates that the learning process will always draw several unlabeled data from a set \tilde{X} of unlabeled data. When p is set to 0, it indicates that the learning process will not draw any unlabeled data. In other

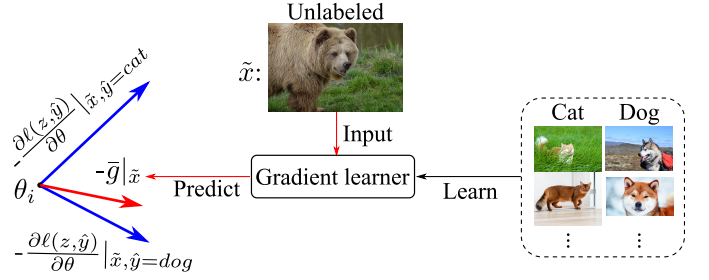


Figure 4: Comparison between the predicted gradient \bar{g} and the gradients $\frac{\partial \ell(z, \hat{y})}{\partial \theta}$ generated with pseudo labels \hat{y} . Assume the proposed gradient learner is trained with the samples in categories cat and dog, given an unlabeled image \tilde{x} , the proposed gradient learner would take all learned class-specific knowledge (i.e. w.r.t categories cat and dog) into account, instead of taking one category (i.e. cat or dog) into account in pseudo labeling methods.

words, p manages the transition from supervised continual learning to SSCL.

The process of predicting gradients is described in lines 11–14 in Algorithm 1.

4.3 Connection to Pseudo Labeling

Note that we do not assume that the underlying classes that are associated with the unlabeled data are the same as or similar to the known classes. As a result, the distributions of the unlabeled samples could be very different from the labeled samples. Hence, directly predicting pseudo label for back-propagation may not be suitable in the SSCL setting.

When labels are unavailable, a common practice to leverage unlabeled samples is by training a teacher model with labeled samples and then predicting pseudo labels on unlabeled samples [19], [31], [36], [41]. Pseudo labeling [19], [31], [41] is viewed as a teacher-student learning framework, i.e.

$$\underset{\theta'}{\text{minimize}} \quad \ell(f_{\theta'}^{tch}(x_i, t_i), y_i) \quad (13)$$

$$\hat{y} = \arg \max_j [f_{\theta'}^{tch}(\tilde{x}, t_i)]_j \quad (14)$$

$$\underset{\theta}{\text{minimize}} \quad \ell(f_{\theta}^{stn}(x_i, t_i), \hat{y}) \quad (15)$$

where *tch* (resp. *stn*) stands for teacher (resp. student), θ' (resp. θ) are the weights of the teacher (resp. student), $((x_i, t_i), y_i)$ is a labeled sample, and \tilde{x} is an unlabeled sample. In short, the teacher would be trained with labeled samples by Eq. (13). When it comes across unlabeled sample \tilde{x} , the teacher first predicts an one-hot pseudo label \hat{y} by Eq. (14) and then \hat{y} is viewed as the label for training the student by Eq. (15). A common alternative to one-hot pseudo labels in Eq. (14) is the probabilities w.r.t. each class, which is used in leveraging unlabeled data in the class-incremental learning [31]. To generate probabilistic labels, the softmax function is usually applied. We denote the one-hot pseudo labeling method and the probabilistic pseudo labeling method as *1-PL* and *P-PL* for simplicity.

The difference between gradient prediction and pseudo labeling is shown in Fig. 4. As teacher models have a chance of generating incorrect labels, the resulting gradients would

vary with different pseudo labeling. Instead, the proposed gradient learner is trained with labeled samples so the predicted gradients are generated with implicit knowledge that maps visual appearance to various visual concepts, rather than one. For example, given training samples of cat and dog, when the proposed gradient learner observes a fox image to predict the pseudo gradient, the pseudo gradient would be aligned with the learned knowledge of both cat and dog, instead of only cat or only dog. Therefore, the pseudo gradients generated by the proposed gradient learner have better generalizability than the ones generated by pseudo labeling methods. Last but not least, as indicated in Eq. (7), the predicted gradients are generated to minimize the fitness loss, while the gradients generated by pseudo labeling methods aim to reproduce the gradients generated with ground-truth labels. Ideally, if the pseudo labels are identical to the ground-truth labels, the gradients generated with pseudo labels would be identical to the gradients generated with ground-truth labels. However, this rarely happens in practice as unlabeled data have no labels or the underlying labels are unknown.

On the other hand, each task in SSCL has a limited number of labeled samples and the visual concepts of any two tasks are different. With limited labeled samples, it is difficult to predict correct pseudo labels. Thus, predicting pseudo gradients is more straightforward and effective in this case.

Furthermore, pseudo labeling methods have many more parameters than the proposed gradient learner. Although the outputs of the teacher model and the proposed gradient learner are supposed to be of the same dimension, the inputs are different. The former takes images as input whereas the latter takes continual learning models' output as input. Thus, the teacher models usually have the same as or more parameters ($> 1M$) than the student models [17], [19], [31], whereas the proposed gradient learner is a small MLP with fewer parameters ($< 10K$)

4.4 Geometric Interpretation

Fig. 5 shows the geometric interpretation of gradient prediction by comparing SSL (bottom) with supervised learning (top). In this illustrative example, given two labeled images, s_1 and s_2 , and one unlabeled image, \tilde{x}_1 , the predicted gradient $-\bar{g}|\tilde{x}_1$ helps boost the convergence, i.e. θ'_{i+2} is closer to the underlying local minimum θ^* than θ_{i+2} . This also impacts on the generalizability. Given an unseen labeled triplet (x, t, y) , we have inequality $\ell(f(x; \theta'_{i+2}), t, y) < \ell(f(x; \theta_{i+2}), t, y)$. This implies that the continual learning model with pseudo gradients is likely to be closer to a local minimum than the one that is not using it.

4.5 Trade-off: Overwhelming vs. Generalizing

It is desirable to use as many unlabeled data as possible, as long as the data improve the generalizability of the continual learning models. Unfortunately, this goal is difficult to achieve. The reasons are two-fold. Firstly, as shown in Fig. 2, since the underlying class of the unlabeled images are unknown, the distributions of unlabeled data could be considerably different from the ones of the labeled data. Secondly, gradient learning and prediction are challenging

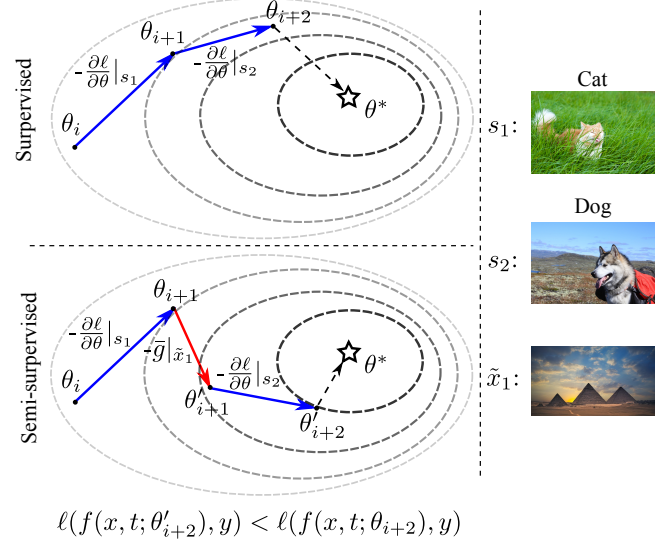


Figure 5: Geometric interpretation of supervised learning (top) and semi-supervised learning (bottom). Through leveraging the semantics of unlabeled images, the generalizability of models is expected to be improved. Experimental results in Table 3–7 validate this finding.

as it is a regression task in a high-dimensional space and the values of gradients are usually small but influential. Last but not least, in contrast to classification task, where the labels are one-hot vectors that are in $[0, 1]$, the ranges of vanilla gradients are determined by the labeled data and lie in $(-\infty, +\infty)$. Therefore, gradient learning task is by nature very challenging.

As a result, when more unlabeled data are used in the learning process, it is more prone to accumulate prediction errors that harm the training quality. Specifically, predictive errors in the back-propagation could overwhelm the knowledge learned from the given labeled data. Therefore, achieving a good trade-off between overwhelming and generalizing is important in the SSCL problem. In this work, we use a probabilistic threshold p to implement this trade-off.

5 EXPERIMENT

5.1 Experimental Set-up

We follow the experimental protocols used in GEM [8] and ACL [7]. In the training scheme of GEM, the models will observe training samples and no training samples will be observed for a second time. The training and test samples are randomly assigned to n tasks according to classes and each task has training and test samples with different classes from the other tasks. Similar to GEM, ACL randomly assigns the samples into n tasks, but in each task, there are multiple epochs that repeat the stochastic process over the training samples as the conventional supervised learning. After the training on every task is done, the trained models would be evaluated with all the test samples of all tasks, including the tasks that the continual learning process has gone through and the tasks which have not been executed yet. Furthermore, to understand the generalization ability of the proposed method in SSL task, we follow the experimental protocols used in [20] to evaluate the proposed method.

5.2 Datasets

In the GEM training scheme, we use the following datasets. **MNIST permutation (MNIST-P)** [25] is a variant of MNIST [65], which consists of 70000 images of size 28×28 . Each image is transformed by a fixed permutation of pixels. **MNIST rotation (MNIST-R)** [8] is similar to MNIST-P, but each image is rotated by a fixed angle between 0 and 180 degrees. **Incremental CIFAR-100 (iCIFAR-100)** [26] is a variant of the CIFAR-100 [66], which consists of 60000 images of size 32×32 . The images are split into multiple subsets by the classes.

In the ACL training scheme, we use **CIFAR-100** [7] and **miniImageNet** [67]. CIFAR-100 is also split into multiple subsets like iCIFAR-100. Instead of being used once, the images in each task are repeatedly used in every epoch. miniImageNet is a variant of ImageNet [15], which consists of 60000 images of size 84×84 with 100 classes.

Following GEM and ACL, all training samples are split into 20 tasks. Briefly, each task on iCIFAR-100, CIFAR-100, and miniImageNet has 5 classes. For MNIST-P and MNIST-R, each task has 10 classes and is performed with different permutation or rotation from the other tasks.

For the experiments on MNIST-R, MNIST-P, iCIFAR-100, and CIFAR-100, we use Tiny ImageNet as unlabeled dataset. For the experiments on miniImageNet, we use the unlabeled images from MS COCO [68]. Both ImageNet and MS COCO are widely-used large-scale real-world datasets. Therefore, the unlabeled images are representative and general for various continual learning tasks.

In the semi-supervised training scheme, we follow the same experimental protocols used in [20] to evaluate the proposed method on SVHN [69], CIFAR-10, and CIFAR-100 [66]. The numbers of labeled data are 1k, 4k, and 10k for SVHN, CIFAR-10, and CIFAR-100, respectively.

5.3 Metrics & Methods

To comprehensively validate the performance of the proposed method, we conduct experiments based on the training schemes of GEM and ACL. DCL [9] achieves state-of-the-art performance on MNIST-P, MNIST-R and iCIFAR-100, and is considered as another baseline in the GEM training scheme.

Continual learning has three key metrics, namely average accuracy (ACC), backward transfer (BWT), and forward transfer (FWT) [8], *i.e.*

$$ACC = \frac{1}{T} \sum_{i=1}^T R_{T,i} \quad (16)$$

$$BWT = \frac{1}{T-1} \sum_{i=1}^{T-1} R_{T,i} - R_{i,i} \quad (17)$$

$$FWT = \frac{1}{T-1} \sum_{i=2}^T R_{i-1,i} - \bar{b}_i \quad (18)$$

where R is the test classification accuracy, T is the number of tasks, and \bar{b}_i is the test classification accuracy at random initialization at the i -th task. Average accuracy indicates the predictive ability of the trained models on all tasks. BWT measures the effect of how learning a task t influences the performance on previous tasks $k < t$. Large negative

TABLE 1: Hyperparameters w.r.t. the proposed method in the SSCL setting. BS denotes batch size of unlabeled images.

Dataset	Method	Backbone	BS	p	α	λ	h_ω
MNIST-R	GEM	MLP	4	0.15	0.001	0.30	(64,16)
MNIST-R	DCL	MLP	4	0.15	0.001	0.30	(64,16)
MNIST-P	GEM	MLP	4	0.15	0.001	0.50	(64,16)
MNIST-P	DCL	MLP	4	0.15	0.001	0.49	(64,16)
iCIFAR-100	GEM	ResNet-18	4	0.30	0.005	2.00	(128,32)
iCIFAR-100	DCL	ResNet-18	4	0.30	0.005	2.50	(128,32)
iCIFAR-100	GEM	EffNet-B1	4	0.20	0.005	2.00	(128,32)
iCIFAR-100	DCL	EffNet-B1	4	0.35	0.005	2.00	(128,32)
CIFAR-100	ACL	AlexNet	64	0.30	0.001	0.20	(128,32)
miniImageNet	ACL	AlexNet	64	0.35	0.001	0.15	(128,32)

TABLE 2: Hyperparameters w.r.t. the proposed method in the SSL setting. We follow [20] for the hyperparameters that are not specific to the proposed method.

Dataset	Backbone	α	λ	h_ω
SVHN	Conv-Large [70]	0.001	2.00	(128,32)
CIFAR-10	Conv-Large	0.001	1.00	(128,32)
CIFAR-100	Conv-Large	0.001	1.00	(128,32)

score is referred as catastrophic forgetting while positive score implies that learning new tasks generalizes to previous tasks. Correspondingly, FWT measures the effect of how learning a task t influences the performance on future tasks $k > t$. Positive score implies that learning a task generalizes to future tasks, which is similar to zero-shot learning. In the ACL training scheme, we use the same metrics, *i.e.* average accuracy and BWT, as [7]. We denote a baseline as *backbone* (if any) *continual algorithm*, *e.g.* ResNet GEM. Similarly, we denote the proposed method as *backbone* (if any) *continual algorithm* + proposed, which indicates the proposed method is used to leverage the information from unlabeled images. Also, following [31] and [20], we report the performance of 1-PL, P-PL, and MG for the purpose of comparison in the continual learning setting. Specifically, the teacher model takes images as input to predict pseudo labels when the learning process encounters unlabeled images. The teacher model is composed by the same backbone of the continual learning model and a linear transformation layer that generate pseudo labels in each task. In other words, 1-PL and P-PL have many more parameters than the baseline and the proposed method.

5.4 Hyperparameters & Implementation Details

We use the same training hyperparameters in GEM [8], DCL [9], and ACL [7]. More details can be found in these works or in our code repository. Here, we focus on the hyperparameters that are related to the proposed method. There are five hyperparameters, namely threshold p , magnitude ratio α , loss scale λ , network architecture h_ω , and batch size of unlabeled images. The hyperparameters w.r.t. the proposed method used in the SSCL and SSL setting are reported in Table 1 and Table 2, respectively. In particular, we follow [20] to use the unlabeled data with $p = 1.0$ in SSL.

Specifically, this work follows the same experimental protocol used in [8], [9] to evaluate the proposed method on MNIST-R, MNIST-P, and iCIFAR-100, while it follows

TABLE 3: Performances on MNIST-R. All methods use MLP as the backbone network [8], [9]. The proposed gradient learner has 1824 parameters. Accuracy is in (%). The top performance is highlighted in bold. MG and PG stand for meta gradient [20] and predicted gradient (proposed), respectively. FT and COS indicate the fitness loss and the cosine similarity loss, respectively.

Methods	Accuracy	BWT	FWT
EWC [25]	54.61	-0.2087	0.5574
GEM [8]	83.35	-0.0047	0.6521
DCL [9]	84.08	0.0094	0.6423
GEM + 1-PL	74.58	-0.0782	0.6319
GEM + P-PL	79.39	-0.0380	0.6453
GEM reproduced	83.03	-0.0061	0.6482
GEM + MG	84.97	0.0051	0.6552
GEM + proposed	86.54	0.0227	0.6537
DCL + 1-PL	82.12	0.0022	0.6275
DCL + P-PL	83.34	0.0033	0.6359
DCL reproduced	84.88	0.0088	0.6526
DCL + MG	85.74	0.0168	0.6518
DCL + proposed	86.26	0.0106	0.6620

the same experimental protocol used in [7] to evaluate the proposed method on CIFAR-100 and miniImageNet. All hyperparameters that are used with the baselines are used with the proposed method as well.

Without loss of generality, we use MLP as the gradient learner $h(\cdot; \omega)$ (h_ω for short). Assume the gradient is in \mathbf{R}^m , we denote (dimension of the 1st layer output, dimension of the 2nd layer output, ..., dimension of the penultimate layer output) for simplicity. For instance, given $m = 5$, architecture (64, 16) indicates the MLP consists of three layers, the first one is a linear operation with a coefficient matrix of size 5×64 , the second one is with a coefficient matrix of 64×16 , and the last one is with a coefficient matrix of size 16×5 .

Similar to other supervised learning methods, few learning steps may not be adequate to train a good gradient learner. Hence, the gradient learner is trained from the very beginning, but the predicted gradients are used after 50 learning steps in the GEM and DCL training scheme, and after 5 learning steps in the ACL training scheme.

Note that restricted to the shared and private module design in ACL [7], which requires a fixed dimension of the input features, the batch size of unlabeled images has to be the same as the batch size of training samples, that is, 64.

5.5 Generalization Performance

In the continual learning setting (*i.e.* Table 3–5), the proposed method consistently improves the average accuracy, BWT, and FWT of the compared baselines. This implies that the proposed method effectively utilizes the information of unlabeled images to improve the predictive ability, alleviates catastrophic forgetting, and enhances zero-shot learning ability. In the adversarial continual learning setting (*i.e.* Table 6 and 7), the average accuracy and BWT of the baseline are improved by the proposed method. Moreover, the standard deviation w.r.t. the proposed method over 5 runs is smaller than the corresponding baseline. This implies the proposed method is more stable than the baseline.

On the other hand, 1-PL and P-PL yield lower accuracies than the proposed method. This is because the pseudo labels

TABLE 4: Performances on MNIST-P. All methods use MLP as the backbone network [8], [9]. The proposed gradient learner has 1824 parameters.

Methods	Accuracy	BWT	FWT
EWC [25]	59.31	-0.1960	-0.0075
GEM [8]	82.44	0.0224	-0.0095
DCL [9]	82.58	0.0402	-0.0092
GEM + 1-PL	80.61	0.0327	-0.0014
GEM + P-PL	80.58	0.0224	-0.0039
GEM reproduced	82.35	0.0251	-0.0101
GEM + MG	82.30	0.0332	-0.0170
GEM + proposed	82.91	0.0316	-0.0072
DCL + 1-PL	81.57	0.0479	0.0002
DCL + P-PL	80.95	0.0219	-0.0083
DCL reproduced	82.83	0.0279	-0.0100
DCL + MG	82.48	0.0423	-0.0078
DCL + proposed	82.97	0.0402	-0.0038

TABLE 5: Performance on iCIFAR-100. *ResNet* indicates ResNet-18. *EffNet* stands for EfficientNet (B1) [59]. The proposed gradient learner has 4896 parameters.

Methods	Accuracy	BWT	FWT
EWC [25]	48.33	-0.1050	0.0216
iCARL [26]	51.56	-0.0848	0.0000
ResNet GEM [8]	66.67	0.0001	0.0108
ResNet DCL [9]	67.92	0.0063	0.0102
EffNet GEM [9]	80.80	0.0318	-0.0050
EffNet DCL [9]	81.55	0.0383	-0.0048
ResNet GEM + 1-PL	65.44	0.0861	-0.0030
ResNet GEM + P-PL	65.55	0.0511	-0.0033
ResNet GEM reproduced	66.92	0.0132	-0.0048
ResNet GEM + MG	67.24	0.0614	-0.0001
ResNet GEM + proposed	68.74	0.0619	0.0055
ResNet DCL + 1-PL	66.43	0.0765	0.0051
ResNet DCL + P-PL	67.78	0.0704	0.0078
ResNet DCL reproduced	67.55	0.0048	-0.0117
ResNet DCL + MG	66.07	0.0524	0.0184
ResNet DCL + proposed	68.53	0.0574	-0.0038
EffNet GEM + 1-PL	78.33	0.0855	-0.0106
EffNet GEM + P-PL	77.46	0.0535	0.0077
EffNet GEM reproduced	81.44	0.0128	0.0105
EffNet GEM + MG	83.95	0.0294	-0.0256
EffNet GEM + proposed	85.51	0.0219	0.0148
EffNet DCL + 1-PL	77.12	0.0862	-0.0160
EffNet DCL + P-PL	76.82	0.0821	0.0097
EffNet DCL reproduced	83.47	0.0266	-0.0185
EffNet DCL + MG	85.06	0.0488	-0.0043
EffNet DCL + proposed	85.70	0.0378	0.0017

TABLE 6: Performance on CIFAR-100 in adversarial continual learning setting. The training process is repeated 5 times, and the average accuracy and standard deviation are reported [7]. ACL uses AlexNet [57] as backbone. The proposed gradient learner has 1427 parameters.

Methods	Accuracy	BWT
A-GEM [5]	54.38±3.84	-0.2199±0.0405
ER-RES [6]	66.78±0.48	-0.1501±0.0111
PNN [27]	75.25±0.04	0
HAT [12]	76.96±1.23	0.0001±0.0002
ACL [7]	78.08±1.25	0±0.0001
ACL reproduced	78.17±1.32	0.01±0.0168
ACL + proposed	78.46±1.05	0.01±0.0123

are likely to be incorrect as the training samples are not adequate and the visual concepts vary from task to task

TABLE 7: Performances on miniImageNet in adversarial continual learning setting. The training process is repeated 5 times, and the average accuracy and standard deviation are reported [7]. ACL uses AlexNet [57] as backbone. The proposed gradient learner has 1427 parameters.

Methods	Accuracy	BWT
A-GEM [5]	52.43±3.10	-0.1523±0.0145
ER-RES [6]	57.32±2.56	-0.1134±0.0232
PNN [27]	58.96±3.50	0
HAT [12]	59.45±0.05	-0.0004±0.0003
ACL [7]	62.07±0.51	0±0
ACL reproduced	62.69±1.01	0±0.0042
ACL + proposed	63.88±0.39	0±0.0000

TABLE 8: Semi-supervised classification error rates (%) of the Conv-Large [70] architecture on the SVHN, CIFAR-10, and CIFAR-100 datasets. The numbers of labeled data are 1k, 4k, and 10k for these three datasets, respectively. We follow the exact experimental protocol used in [20] and use the official implementation code to conduct this experiment. The meta-objective defined in [20] is used as the fitness loss to learn to predict pseudo gradients for unlabeled images.

Method	SVHN	CIFAR-10	CIFAR-100
Co-training [71]	3.29	8.35	34.63
TNAR-VAE [72]	3.74	8.85	-
ADA-Net [73]	4.62	10.30	-
DualStudent [74]	-	8.89	32.77
MG [20]	3.15	7.78	30.74
MG reproduced	3.53	7.82	30.74
MG + proposed	3.45	7.46	30.02

(the analysis of pseudo labeling is provided in Section 6). Incorrect pseudo labels lead to the gradients that guide the learning process in unpredictable directions. Note that the BWTs of 1-PL and P-PL are higher than the others. This results from lower accuracy. As indicated in the definition of BWT (Eq. (17)), when the test classification accuracy $R_{i,i}$ on the i -th task with the model trained in the i -th task is low, it will lead to high BWT. In other words, when overall ACC is high, BWT tends to be relatively low. Similarly, FWT tends to be high (*i.e.* 0.0216) when the corresponding accuracies over tasks are low (*i.e.* 48.33%).

Since the proposed method is generic, we also evaluate it in the SSL setting [20]. The meta-objective defined in [20] is used as the fitness loss to learn to predict pseudo gradients for unlabeled images. The experimental results on SVHN [69], CIFAR-10, and CIFAR-100 are reported in Table 8. The proposed method can improve the performance of the SSL task. This implies that the proposed method generally work with the unlabeled data with the pseudo labels that share the same or similar distributions as the labeled data.

6 ANALYSIS

This section provides a series of experiments to analyze the proposed method. All analyses are based on iCIFAR-100.

6.1 Effects of Visual Diversity

Here, we study the influence of the variance between training images and the unlabeled images on the model

TABLE 9: Effects of visual diversity of \tilde{x} on the classification performance (%) on iCIFAR-100 with ResNet GEM.

Source	Accuracy	BWT	FWT
$\tilde{x} = \emptyset$	66.92	0.0132	-0.0048
Tiny ImageNet [15]	68.74	0.0619	0.0055
MS COCO [68]	67.78	0.0562	0.0006
CUB-200 [75]	68.03	0.0460	0.0041
FGVC-aircraft [76]	67.05	0.0385	0.0159
Stanford-cars [77]	67.41	0.0465	-0.0028

performance. In addition to the Tiny ImageNet from the previous section, we selected a variety of datasets, namely MS COCO [68], CUB-200 [75], FGVC-aircraft [76], and Stanford-cars [77], as the source of unlabeled images. The classes in these datasets overlap with the ones in CIFAR-100 to various degrees. The performance are reported in Table 9. Overall, the proposed method shows improvement with all unlabeled images source. The images in Tiny ImageNet are similar to the ones in MS COCO, where both are natural images but having different image resolution. The resolution of images in Tiny ImageNet is closer to that in CIFAR-100 than MS COCO. Therefore, using Tiny ImageNet images leads to the most performance improvement. In contrast, the images in FGVC-aircraft are the most dissimilar to the ones in CIFAR-100 and the accuracy improvement is marginal. On the other hand, using CUB-200 leads to higher accuracy than using MS COCO. This is because CUB-200 shares similar visual concepts with CIFAR (*i.e.* bird) and both the two datasets are object-centered, whereas the images of MS COCO contain multiple objects and are non-object-centered.

6.2 Using Random Noise as Pseudo Gradients

To evaluate the efficacy of the proposed method, we use random noise as the predicted gradients. The random noise is either generated by a uniform distribution $\mathcal{U}(-1, 1)$ or a normal distribution $\mathcal{N}(0, 1)$. The results with the same experimental set-up as Table 5 are shown in Table 10. Specifically, $\mathcal{U}(-1, 1)$ or $\mathcal{N}(0, 1)$ indicates that the noise is used as $\bar{g}|_{\tilde{x}_i}$ (see line 13 in Algorithm 1), while *proposed* indicates that the corresponding noise is used as $g|_{\tilde{x}_i}$ (see line 12 in Algorithm 1) and they will be the input to the equations in line 13 in Algorithm 1. As shown, $\mathcal{U}(-1, 1)$ or $\mathcal{N}(0, 1)$ produces much lower accuracy than the other settings. Note that the random noise disturbs the training for all the tasks so that the accuracies of preceding tasks are low when computing the BWT scores for the current task. As discussed in Section 5.5, this leads to high BWTs, according to the definition of BWT (Eq. (17)).

6.3 Effects of Number of Labeled/Unlabeled Images

To understand how the numbers of labeled and unlabeled images affect the performance of continual learning, we conduct an analysis to show the performance of using different amount (range from 0% to 100%) of labeled and unlabeled images. Without using any unlabeled images, it implies the methods is a regular supervised continual learning method. We compare our proposed method with Meta-gradient [20] and the results with different amount of labeled (unlabeled) images are reported in Table 11 (Table 12). For results in

TABLE 10: Effects of random noise on the performance (%) with ResNet GEM. The noise follows a uniform distribution $\mathcal{U}(-1, 1)$ or a unit normal distribution $\mathcal{N}(0, 1)$, and is used as predicted gradients. The experimental details are described in Section 6.2.

Setting	Accuracy	BWT	FWT
No noise	66.92	0.0132	-0.0048
No noise + proposed	68.74	0.0619	0.0055
$\mathcal{U}(-1, 1)$	54.10	0.1978	-0.0121
$\mathcal{U}(-1, 1)$ + proposed	67.71	0.0533	0.0004
$\mathcal{N}(0, 1)$	45.29	0.2121	0.0032
$\mathcal{N}(0, 1)$ + proposed	67.08	0.0502	0.0007

TABLE 11: Effects of different numbers of labeled images on iCIFAR-100. *L-Ratio* indicates the amount of labeled images in iCIFAR-100 used for training. About 20% of unlabeled images are sampled from Tiny ImageNet. The setting is the same as the one used in Table 5 and ResNet GEM is used in this analysis.

Method	L-Ratio	Accuracy	BWT	FWT
MG [20]	20%	48.02	0.0420	0.0033
	40%	60.09	0.0822	-0.0004
	60%	61.40	0.0699	-0.0047
	80%	63.21	0.0541	0.0006
	100%	67.24	0.0614	-0.0001
Proposed	20%	50.38	0.0693	-0.0011
	40%	61.10	0.1045	-0.0039
	60%	61.38	0.0582	0.0107
	80%	64.60	0.0552	0.0003
	100%	68.74	0.0619	0.0055

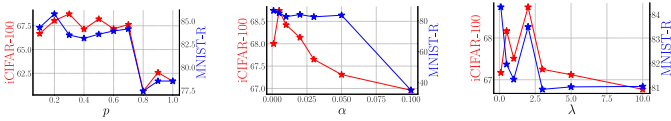


Figure 6: Effects of p (left), α (middle), and λ (right) on accuracy across datasets (i.e. iCIFAR-100 and MNIST-R).

Table 11, we use 20% of unlabeled images for training. An observation is that the performance increases as more labeled images are used for training. On the contrary, using more unlabeled images, which follows very different distributions in comparison to the labeled images, does not always lead to better performance. As discussed in Section 4.5 and shown in Fig. 2, the distributions of unknown classes' samples could be very different from the ones of known classes' samples. Therefore, using more unlabeled images of the unknown classes would lead to a performance drop.

6.4 How Hyperparameters Range Across Datasets

In this section, we study how key hyperparameters p , α , and λ are robust to the training on different datasets when using the same unlabeled data. Fig. 6 shows the curves of the accuracy w.r.t. p , α , and λ . Overall, the curves w.r.t. iCIFAR-100 and MNIST-R are similar to each other. Specifically, as the values of p , α , and λ exceed a certain point, it would lead to a significant drop in accuracy. The parameters used in this work (see Fig. 1) are selected in the optimal range.

TABLE 12: Effects of different numbers of unlabeled images on iCIFAR-100. *U-Ratio* is the amount of unlabeled images in Tiny ImageNet used for training. The setting is the same as the one used in Table 5 and ResNet GEM is used in this analysis.

Method	U-Ratio	Accuracy	BWT	FWT
MG [20]	0%	66.92	0.0132	-0.0048
	10%	66.43	0.0539	-0.0118
	20%	67.24	0.0614	-0.0001
	40%	67.03	0.0601	-0.0010
	60%	66.95	0.0579	-0.0037
	80%	66.71	0.0536	-0.0059
	100%	66.27	0.0456	0.0018
Proposed	0%	66.92	0.0132	-0.0048
	10%	67.80	0.0525	0.0084
	20%	68.74	0.0619	0.0055
	40%	67.53	0.0630	0.0140
	60%	67.99	0.0644	0.0099
	80%	67.91	0.0581	-0.0021
	100%	66.96	0.0573	0.0000

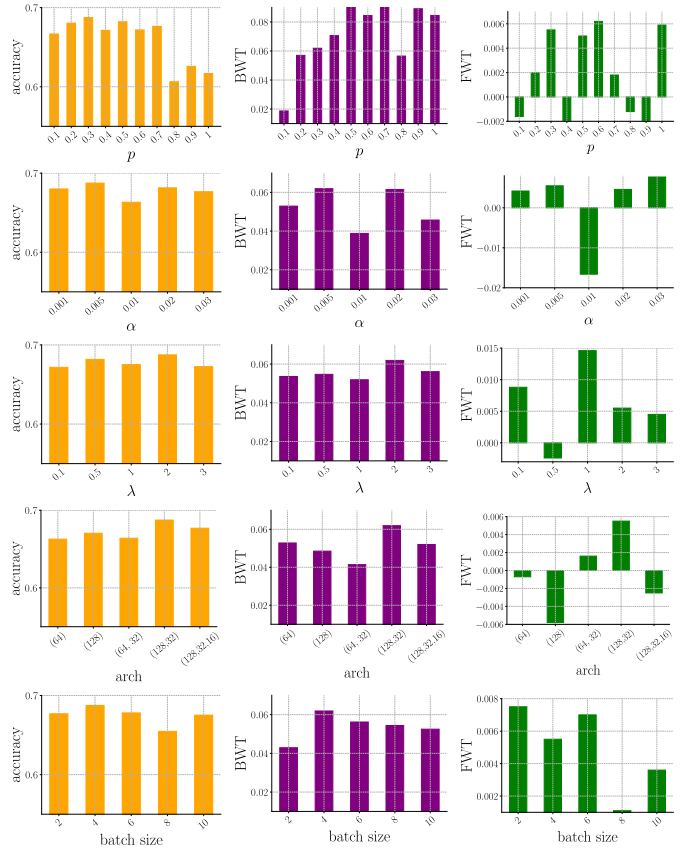


Figure 7: Ablation study of the proposed method with various hyperparameters detailed in Section 5. The metrics are classification accuracy (left), BWT (middle), and FWT (right). ResNet GEM is used for the analysis.

6.5 Ablation Study

As introduced in the experimental set-up, the proposed method depends on five hyperparameters. This section shows the corresponding ablation studies and the results are shown in Fig. 7. As discussed in Section 4, p reflects the trade-off between overwhelming and generalizing. As p in-

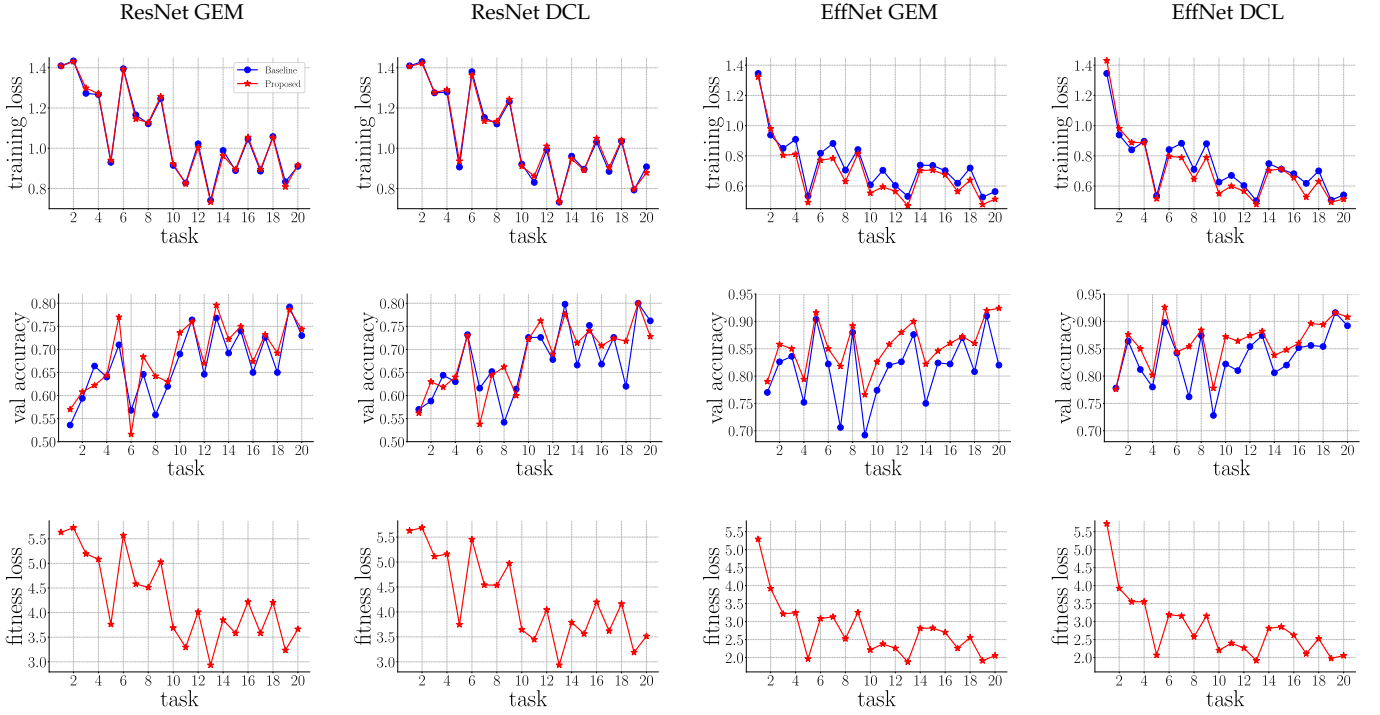


Figure 8: Plots of the training loss curves (top row), the validation accuracy curves (middle row), and fitness loss curves (bottom row) on iCIFAR-100 with various pairs of methods and backbones.

creases, the accuracy drops significantly. This is as expected in the earlier discussion. Moreover, we can observe that the architecture of the proposed gradient learner is more critical to the proposed method in terms of accuracy, BWT, and FWT, comparing to the other hyperparameters.

6.6 Training Loss, Validation Accuracy, and Fitness Loss

The losses and accuracy against tasks are shown in Fig. 8. As shown, the proposed method can improve the predictive ability of continual learning models, *i.e.* EfficientNet GEM and EfficientNet DCL, when unlabeled data and corresponding predicted gradients are used. The loss is decreased and the accuracy is increased. On the bottom row, the curves of the fitness loss vs. task show that the fitness loss (7) across tasks is minimized by the proposed gradient learner.

6.7 Pseudo Labeling vs. Gradient Prediction

This section examine how pseudo labeling and gradient prediction work in the continual learning method. Moreover, we investigate the correlations between the gradients generated by various methods and its performance.

To understanding the efficacy of pseudo labeling methods, we first inspect the gradients generated with pseudo labels and the accuracy of pseudo label prediction on training samples. We take the gradients generated with ground-truth labels as a reference and compute the cosine similarity $\cos(\frac{\partial \ell}{\partial z}|_{x,t,y}, \frac{\partial \ell}{\partial z}|_{x,t,\hat{y}})$ between the gradients generated with two types of labels, where x, t, y are training samples and \hat{y} are pseudo labels. In this way, the discrepancy can be quantified as the cosine similarity. In other words, if pseudo labels are the same as the ground-truth labels, the cosine

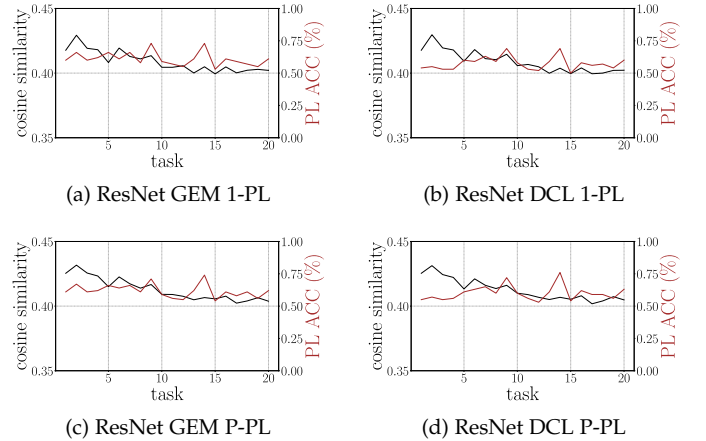


Figure 9: Plots of cosine similarity between the gradients generated with ground-truth labels and pseudo labels (black curve), as well as the corresponding pseudo label prediction accuracy (brown curve). Due to the lack of training samples and the dynamical change of visual concepts at each task, the pseudo label prediction perform badly (lower than 1%). This is consistent with the drop on the cosine similarity, which should be 1 if the predicted pseudo labels are correct.

similarity between the gradients generated with pseudo labels and ground-truth labels should be 1, which indicates the resulting gradients are fully aligned. As shown in Fig. 9, the cosine similarities generated by 1-PL and P-PL are stably around 0.4. The drop from 1 to 0.4 results from the incorrect pseudo labels. The accuracies of 1-PL and P-PL are lower than 1%. The reasons for the low accuracy are two-fold. First, in continual learning, all samples are only observed

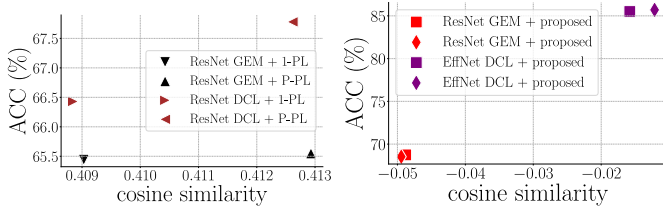


Figure 10: Correlation between cosine similarity and averaged accuracy. Left: Experiments with 1-PL and P-PL; Right: Experiments with the proposed method.

once and the number of training sample w.r.t. a class is relatively small, *e.g.* 500 on iCIFAR-100. Thus, there is not enough data to train a high-performance teacher model. Second, the classes of samples are used for training at a task are distinct from that of the other tasks. This dynamic results in the difficulty to train a strong teacher model.

Next, we examine how the gradients generated by various methods correlate to the performance. Note that the predicted gradients aim to minimize the fitness loss (7), while the pseudo labeling methods aim to maximize the similarity between the gradients generated with pseudo labels and ground-truth gradients labels. Hence, the predicted gradients are expected to differ from the ground-truth generated gradients. As shown in Fig. 10, ResNet GEM + P-PL yields a higher cosine similarity than ResNet DCL + P-PL, but achieves a lower accuracy. In contrast, the proposed method's (*i.e.* with gradient prediction) accuracy is clearly proportional to the cosine similarity. On the other hand, we observe that discriminative features produced by a strong backbone will lead to better predicted gradients in terms of the geometric relationship.

7 CONFUSION MATRIX

To comprehensively understand the efficacy of the proposed predicted gradients, we visualize the confusion matrices generated by various methods on iCIFAR-100 in Fig. 11 and 12. The i -th row of the confusion matrix indicates the test classification accuracies over 20 tasks with the model trained on the i -th task. Similarly, the j -th column indicates the results are evaluated on the test set of the j -th task.

As shown in Fig. 11, leveraging extra unlabeled images with the proposed method will have lower accuracies on early tasks than the baseline as the proposed gradient learner does not have sufficient training samples for learning. With more and more training samples being observed, better predicted gradients are yielded to improve the performance on late tasks. In addition, the accuracies of 1-PL and P-PL are overall lower due to the disturbance caused by the incorrect pseudo labels. As discussed in Section 5.5, low $R_{i,i}$ leads to a high BWT score.

Table 10 shows that using random noise as predicted gradients yields higher BWT than the other settings. Again, this is because the random noise disturbs the learning process, which leads to low accuracies (see Fig. 12). More importantly, Fig. 12 shows that random noise + proposed is more robust than method with only random noise.

8 CONCLUSION

In this work, we study how to exploit the semantics of the unlabeled data to improve the generalizability of continual learning methods. To this end, we propose a new semi-supervised continual learning method, where a novel gradient learner is trained with labeled data and utilized to generate pseudo gradients when the input label is absent. The proposed method is evaluated in the continual learning and adversarial continual learning settings. The experimental results show that the average accuracy and backward transfer are both improved by the proposed method and achieves the state-of-the-art performance. This implies that leveraging the semantics of the unlabeled data improves the generalizability of the model and alleviates catastrophic forgetting. Last but not least, we provide empirical evidence to show that the proposed method can generalize to the semi-supervised learning task.

ACKNOWLEDGMENTS

This research was funded in part by the NSF under Grants 1908711, 1849107, and in part supported by the National Research Foundation, Singapore under its Strategic Capability Research Centres Funding Initiative. Any opinions, findings and conclusions or recommendations expressed in this material are those of the author(s) and do not reflect the views of National Research Foundation, Singapore.

REFERENCES

- [1] M. B. Ring, "Continual learning in reinforcement environments," Ph.D. dissertation, University of Texas at Austin, 1994.
- [2] S. Thrun, "A lifelong learning perspective for mobile robot control," in *Proceedings of IEEE/RSJ International Conference on Intelligent Robots and Systems*, 1994, pp. 23–30.
- [3] J. C. Schlimmer and D. Fisher, "A case study of incremental concept induction," in *AAAI*, vol. 86, 1986, pp. 496–501.
- [4] M. McCloskey and N. J. Cohen, "Catastrophic interference in connectionist networks: The sequential learning problem," *Psychology of Learning and Motivation*, vol. 24, pp. 109–165, 1989.
- [5] A. Chaudhry, M. Ranzato, M. Rohrbach, and M. Elhoseiny, "Efficient lifelong learning with a-GEM," in *International Conference on Learning Representations*, 2019.
- [6] A. Chaudhry, M. Rohrbach, M. Elhoseiny, T. Ajanthan, P. K. Dokania, P. H. Torr, and M. Ranzato, "On tiny episodic memories in continual learning," in *Workshop on Multi-Task and Lifelong Reinforcement Learning, ICML*, 2019.
- [7] S. Ebrahimi, F. Meier, R. Calandra, T. Darrell, and M. Rohrbach, "Adversarial continual learning," in *European Conference on Computer Vision*, ser. Lecture Notes in Computer Science, vol. 12356, 2020, pp. 386–402.
- [8] D. Lopez-Paz and M. Ranzato, "Gradient episodic memory for continual learning," in *Advances in Neural Information Processing Systems*, 2017, pp. 6467–6476.
- [9] Y. Luo, Y. Wong, M. Kankanhalli, and Q. Zhao, "Direction concentration learning: Enhancing congruency in machine learning," *IEEE Transactions on Pattern Analysis and Machine Intelligence*, pp. 1–1, 2019.
- [10] C. V. Nguyen, Y. Li, T. D. Bui, and R. E. Turner, "Variational continual learning," in *International Conference on Learning Representations*, 2018.
- [11] M. Riemer, I. Cases, R. Ajemian, M. Liu, I. Rish, Y. Tu, , and G. Tesauro, "Learning to learn without forgetting by maximizing transfer and minimizing interference," in *International Conference on Learning Representations*, 2019.
- [12] J. Serra, D. Suris, M. Miron, and A. Karatzoglou, "Overcoming catastrophic forgetting with hard attention to the task," in *International Conference on Machine Learning*, ser. Proceedings of Machine Learning Research, vol. 80, 2018, pp. 4555–4564.

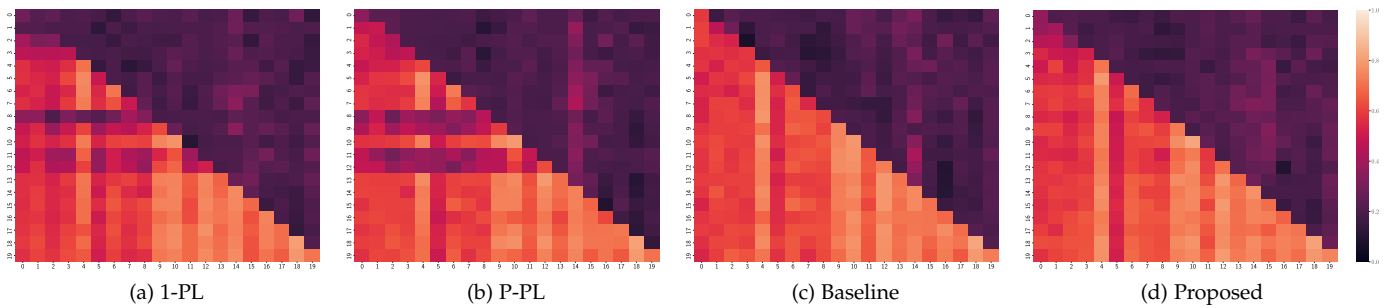


Figure 11: Confusion matrix generated by different methods. The i -th row indicates it is the training stage with the i -th task's samples, while the i -th row j -th column indicates the model trained with the i -th task's samples is evaluated on the j -th task. ResNet GEM is used for the analysis.

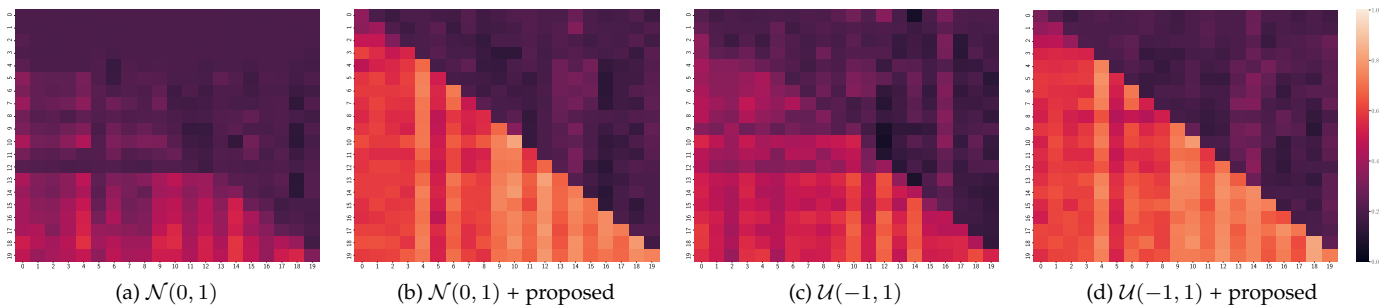


Figure 12: Confusion matrix generated with random noise. The experimental details are described in Section 6.2.

- [13] H. Shin, J. K. Lee, J. Kim, and J. Kim, "Continual learning with deep generative replay," in *Advances in Neural Information Processing Systems*, 2017, pp. 2990–2999.
- [14] S. Sinha, S. Ebrahimi, and T. Darrell, "Variational adversarial active learning," in *IEEE/CVF International Conference on Computer Vision*, 2019, pp. 5972–5981.
- [15] J. Deng, W. Dong, R. Socher, L.-J. Li, K. Li, and L. Fei-Fei, "ImageNet: A large-scale hierarchical image database," in *IEEE Conference on Computer Vision and Pattern Recognition*, 2009, pp. 248–255.
- [16] T. Chen, S. Kornblith, M. Norouzi, and G. Hinton, "A simple framework for contrastive learning of visual representations," in *International Conference on Machine Learning*, ser. Proceedings of Machine Learning Research, vol. 119, 2020, pp. 1597–1607.
- [17] T. Chen, S. Kornblith, K. Swersky, M. Norouzi, and G. Hinton, "Big self-supervised models are strong semi-supervised learners," in *Advances in Neural Information Processing Systems*, 2020.
- [18] D.-H. Lee, "Pseudo-label: The simple and efficient semi-supervised learning method for deep neural networks," in *Workshop on Challenges in Representation Learning, ICML*, vol. 3, no. 2, 2013.
- [19] Q. Xie, M.-T. Luong, E. Hovy, and Q. V. Le, "Self-training with noisy student improves imagenet classification," in *Proceedings of the IEEE/CVF Conference on Computer Vision and Pattern Recognition*, 2020, pp. 10 687–10 698.
- [20] X. Zhang, H. Jia, T. Xiao, M.-M. Cheng, and M.-H. Yang, "Semi-supervised learning with meta-gradient," in *AISTATS*, 2021.
- [21] S. Thrun, "Lifelong learning algorithms," in *Learning to learn*. Springer, 1998, pp. 181–209.
- [22] L. Bottou and Y. Cun, "Large scale online learning," in *Advances in Neural Information Processing Systems*, S. Thrun, L. Saul, and B. Schölkopf, Eds., vol. 16. MIT Press, 2004.
- [23] T. Anderson, *The theory and practice of online learning*. Athabasca University Press, 2008.
- [24] S. C. Hoi, J. Wang, and P. Zhao, "Libol: A library for online learning algorithms," *Journal of Machine Learning Research*, vol. 15, no. 15, pp. 495–499, 2014.
- [25] J. Kirkpatrick, R. Pascanu, N. Rabinowitz, J. Veness, G. Desjardins, A. A. Rusu, K. Milan, J. Quan, T. Ramalho, A. Grabska-Barwinska, D. Hassabis, C. Clopath, D. Kumaran, and R. Hadsell, "Overcoming catastrophic forgetting in neural networks," *Proceedings of the National Academy of Sciences*, vol. 114, no. 13, pp. 3521–3526, 2017.
- [26] S.-A. Rebuffi, A. Kolesnikov, G. Sperl, and C. H. Lampert, "iCaRL: Incremental classifier and representation learning," in *IEEE Conference on Computer Vision and Pattern Recognition*, 2017, pp. 5533–5542.
- [27] A. A. Rusu, N. C. Rabinowitz, G. Desjardins, H. Soyer, J. Kirkpatrick, K. Kavukcuoglu, R. Pascanu, and R. Hadsell, "Progressive neural networks," *arXiv preprint arXiv:1606.04671*, 2016.
- [28] F. Zenke, B. Poole, and S. Ganguli, "Continual learning through synaptic intelligence," in *International Conference on Machine Learning*, ser. Proceedings of Machine Learning Research, vol. 70, 2017, pp. 3987–3995.
- [29] A. Chaudhry, N. Khan, P. Dokania, and P. Torr, "Continual learning in low-rank orthogonal subspaces," *Advances in Neural Information Processing Systems*, vol. 33, 2020.
- [30] S. I. Mirzadeh, M. Farajtabar, R. Pascanu, and H. Ghasemzadeh, "Understanding the role of training regimes in continual learning," *arXiv preprint arXiv:2006.06958*, 2020.
- [31] K. Lee, K. Lee, J. Shin, and H. Lee, "Overcoming catastrophic forgetting with unlabeled data in the wild," in *IEEE/CVF International Conference on Computer Vision*, 2019, pp. 312–321.
- [32] J. Zhang, J. Zhang, S. Ghosh, D. Li, S. Tasci, L. Heck, H. Zhang, and C. . Jay Kuo, "Class-incremental learning via deep model consolidation," in *2020 IEEE Winter Conference on Applications of Computer Vision*, 2020, pp. 1120–1129.
- [33] H. Scudder, "Probability of error of some adaptive pattern-recognition machines," *IEEE Transactions on Information Theory*, vol. 11, no. 3, pp. 363–371, 1965.
- [34] B. M. Shahshahani and D. A. Landgrebe, "The effect of unlabeled samples in reducing the small sample size problem and mitigating the hughes phenomenon," *IEEE Transactions on Geoscience and Remote Sensing*, vol. 32, no. 5, pp. 1087–1095, 1994.
- [35] Y. Yang, F. Nie, D. Xu, J. Luo, Y. Zhuang, and Y. Pan, "A multimedia retrieval framework based on semi-supervised ranking and relevance feedback," *IEEE Transactions on Pattern Analysis and Machine Intelligence*, vol. 34, no. 4, pp. 723–742, 2012.
- [36] Y. Li, J. Yang, Y. Song, L. Cao, J. Luo, and L.-J. Li, "Learning from noisy labels with distillation," in *Proceedings of the IEEE International Conference on Computer Vision*, 2017, pp. 1910–1918.

- [37] M. Kang, K. Lee, Y. H. Lee, and C. Suh, "Autoencoder-based graph construction for semi-supervised learning," in *European Conference on Computer Vision*, ser. Lecture Notes in Computer Science, vol. 12369, 2020, pp. 500–517.
- [38] V. S. Lokhande, S. Tasneeyapant, A. Venkatesh, S. N. Ravi, and V. Singh, "Generating accurate pseudo-labels in semi-supervised learning and avoiding overconfident predictions via hermite polynomial activations," in *Proceedings of the IEEE/CVF Conference on Computer Vision and Pattern Recognition*, 2020, pp. 11 435–11 443.
- [39] Z. Ren, R. A. Yeh, and A. G. Schwing, "Not all unlabeled data are equal: Learning to weight data in semi-supervised learning," in *Advances in Neural Information Processing Systems*, 2020.
- [40] K. Sohn, D. Berthelot, N. Carlini, Z. Zhang, H. Zhang, C. Raffel, E. D. Cubuk, A. Kurakin, and C. Li, "FixMatch: Simplifying semi-supervised learning with consistency and confidence," in *Advances in Neural Information Processing Systems*, 2020.
- [41] H. Pham, Z. Dai, Q. Xie, M.-T. Luong, and Q. V. Le, "Meta pseudo labels," *arXiv preprint arXiv:2003.10580*, 2020.
- [42] F. Chollet, "Xception: Deep learning with depthwise separable convolutions," in *Proceedings of the IEEE Conference on Computer Vision and Pattern Recognition*, 2017, pp. 1251–1258.
- [43] M. Andrychowicz, M. Denil, S. Gomez, M. W. Hoffman, D. Pfau, T. Schaul, B. Shillingford, and N. De Freitas, "Learning to learn by gradient descent by gradient descent," in *Advances in Neural Information Processing Systems*, 2016, pp. 3981–3989.
- [44] Y. Chen, M. W. Hoffman, S. G. Colmenarejo, M. Denil, T. P. Lillicrap, M. Botvinick, and N. Freitas, "Learning to learn without gradient descent by gradient descent," in *International Conference on Machine Learning*, ser. Proceedings of Machine Learning Research, vol. 70, 2017, pp. 748–756.
- [45] S. Hochreiter, A. S. Younger, and P. R. Conwell, "Learning to learn using gradient descent," in *International Conference on Artificial Neural Networks*, 2001, pp. 87–94.
- [46] J. Ji, X. Chen, Q. Wang, L. Yu, and P. Li, "Learning to learn gradient aggregation by gradient descent," in *International Joint Conferences on Artificial Intelligence*, 2019, pp. 2614–2620.
- [47] M. Jaderberg, W. M. Czarnecki, S. Osindero, O. Vinyals, A. Graves, D. Silver, and K. Kavukcuoglu, "Decoupled neural interfaces using synthetic gradients," in *International Conference on Machine Learning*. PMLR, 2017, pp. 1627–1635.
- [48] H. Robbins and S. Monro, "A stochastic approximation method," *The Annals of Mathematical Statistics*, pp. 400–407, 1951.
- [49] S. Boyd, S. P. Boyd, and L. Vandenberghe, *Convex optimization*. Cambridge university press, 2004.
- [50] C. Jin, R. Ge, P. Netrapalli, S. M. Kakade, and M. I. Jordan, "How to escape saddle points efficiently," in *International Conference on Machine Learning*, 2017, pp. 1724–1732.
- [51] Y. Carmon, J. C. Duchi, O. Hinder, and A. Sidford, "Accelerated methods for nonconvex optimization," *SIAM Journal on Optimization*, vol. 28, no. 2, pp. 1751–1772, 2018.
- [52] S. Reddi, M. Zaheer, S. Sra, B. Póczos, F. Bach, R. Salakhutdinov, and A. Smola, "A generic approach for escaping saddle points," in *International Conference on Artificial Intelligence and Statistics*, 2018, pp. 1233–1242.
- [53] D. P. Kingma and J. Ba, "Adam: A method for stochastic optimization," in *International Conference on Learning Representations*, 2015.
- [54] G. Hinton, N. Srivastava, and K. Swersky, "Neural networks for machine learning. lecture 6a. overview of mini-batch gradient descent."
- [55] L. Luo, Y. Xiong, and Y. Liu, "Adaptive gradient methods with dynamic bound of learning rate," in *International Conference on Learning Representations*, 2019.
- [56] M. Zhang, J. Lucas, J. Ba, and G. E. Hinton, "Lookahead optimizer: k steps forward, 1 step back," in *Advances in Neural Information Processing Systems*, 2019, pp. 9593–9604.
- [57] A. Krizhevsky, I. Sutskever, and G. E. Hinton, "ImageNet classification with deep convolutional neural networks," in *Advances in Neural Information Processing Systems*, 2012, pp. 1097–1105.
- [58] K. He, X. Zhang, S. Ren, and J. Sun, "Deep residual learning for image recognition," in *IEEE Conference on Computer Vision and Pattern Recognition*, 2016, pp. 770–778.
- [59] M. Tan and Q. V. Le, "EfficientNet: Rethinking model scaling for convolutional neural networks," in *International Conference on Machine Learning*, ser. Proceedings of Machine Learning Research, vol. 97, 2019, pp. 6105–6114.
- [60] Z. Chen, V. Badrinarayanan, C.-Y. Lee, and A. Rabinovich, "Grad-Norm: Gradient normalization for adaptive loss balancing in deep multitask networks," in *International Conference on Machine Learning*, ser. Proceedings of Machine Learning Research, vol. 80, 2018, pp. 794–803.
- [61] T.-Y. Lin, P. Goyal, R. Girshick, K. He, and P. Dollár, "Focal loss for dense object detection," in *IEEE International Conference on Computer Vision*, 2017, pp. 2980–2988.
- [62] R. Zhao, B. Vogel, and T. Ahmed, "Adaptive loss scaling for mixed precision training," *arXiv preprint arXiv:1910.12385*, 2019.
- [63] T. Hastie, R. Tibshirani, and J. Friedman, *The elements of statistical learning: data mining, inference, and prediction*. Springer Science & Business Media, 2009.
- [64] A. Vaswani, N. Shazeer, N. Parmar, J. Uszkoreit, L. Jones, A. N. Gomez, L. Kaiser, and I. Polosukhin, "Attention is all you need," in *Advances in Neural Information Processing Systems*, 2017, pp. 5998–6008.
- [65] Y. LeCun, L. Bottou, Y. Bengio, and P. Haffner, "Gradient-based learning applied to document recognition," *Proceedings of the IEEE*, vol. 86, no. 11, pp. 2278–2324, 1998.
- [66] A. Krizhevsky, "Learning multiple layers of features from tiny images," Master's thesis, University of Toronto, 2009.
- [67] O. Vinyals, C. Blundell, T. Lillicrap, D. Wierstra *et al.*, "Matching networks for one shot learning," in *Advances in Neural Information Processing Systems*, 2016, pp. 3630–3638.
- [68] T.-Y. Lin, M. Maire, S. Belongie, J. Hays, P. Perona, D. Ramanan, P. Dollár, and C. L. Zitnick, "Microsoft COCO: Common objects in context," in *European Conference on Computer Vision*, ser. Lecture Notes in Computer Science, vol. 8693, 2014, pp. 740–755.
- [69] Y. Netzer, T. Wang, A. Coates, A. Bissacco, B. Wu, and A. Y. Ng, "Reading digits in natural images with unsupervised feature learning," 2011.
- [70] A. Tarvainen and H. Valpola, "Mean teachers are better role models: Weight-averaged consistency targets improve semi-supervised deep learning results," in *Advances in Neural Information Processing Systems*, vol. 30. Curran Associates, Inc., 2017.
- [71] S. Qiao, W. Shen, Z. Zhang, B. Wang, and A. L. Yuille, "Deep co-training for semi-supervised image recognition," in *European Conference on Computer Vision*, ser. Lecture Notes in Computer Science, vol. 11219, 2018, pp. 142–159.
- [72] B. Yu, J. Wu, J. Ma, and Z. Zhu, "Tangent-normal adversarial regularization for semi-supervised learning," in *IEEE Conference on Computer Vision and Pattern Recognition*, 2019, pp. 10 676–10 684.
- [73] Q. Wang, W. Li, and L. V. Gool, "Semi-supervised learning by augmented distribution alignment," in *IEEE International Conference on Computer Vision*, 2019, pp. 1466–1475.
- [74] Z. Ke, D. Wang, Q. Yan, J. S. J. Ren, and R. W. H. Lau, "Dual student: Breaking the limits of the teacher in semi-supervised learning," in *IEEE International Conference on Computer Vision*, 2019, pp. 6727–6735.
- [75] C. Wah, S. Branson, P. Welinder, P. Perona, and S. Belongie, "The Caltech-UCSD Birds-200-2011 Dataset," California Institute of Technology, Tech. Rep. CNS-TR-2011-001, 2011.
- [76] S. Maji, J. Kannala, E. Rahtu, M. Blaschko, and A. Vedaldi, "Fine-grained visual classification of aircraft," Tech. Rep., 2013.
- [77] J. Krause, M. Stark, J. Deng, and L. Fei-Fei, "3D object representations for fine-grained categorization," in *IEEE Workshop on 3D Representation and Recognition, ICCV*, 2013.



Yan Luo is currently pursuing a Ph.D. degree with the Department of Computer Science and Engineering at the University of Minnesota. He received a B.Sc. degree in computer science from Xi'an University of Science and Technology. In 2013, he joined the Sensor-enhanced Social Media (SeSaMe) Centre, Interactive and Digital Media Institute, National University of Singapore, as a Research Assistant. In 2015, he joined the Visual Information Processing Laboratory at the National University of Singapore as a Ph.D. Student. He worked in the industry for several years on distributed system. His research interests include computer vision, computational visual cognition, and deep learning.



Yongkang Wong is a senior research fellow at the School of Computing, National University of Singapore. He is also the Assistant Director of the NUS Centre for Research in Privacy Technologies (N-CRiPT). He obtained his BEng from the University of Adelaide and PhD from the University of Queensland. He has worked as a graduate researcher at NICTA's Queensland laboratory, Brisbane, QLD, Australia, from 2008 to 2012. His current research interests are in the areas of Image/Video Processing, Machine

Learning, Action Recognition, and Human Centric Analysis. He is a member of the IEEE since 2009.



Mohan Kankanhalli is the Provost's Chair Professor at the Department of Computer Science of the National University of Singapore. He is the director with the N-CRiPT and also the Dean, School of Computing at NUS. Mohan obtained his BTech from IIT Kharagpur and MS & PhD from the Rensselaer Polytechnic Institute. His current research interests are in Multimedia Computing, Multimedia Security and Privacy, Image/Video Processing and Social Media Analysis. He is on the editorial boards of several

journals. Mohan is a Fellow of IEEE.



Qi Zhao is an assistant professor in the Department of Computer Science and Engineering at the University of Minnesota, Twin Cities. Her main research interests include computer vision, machine learning, cognitive neuroscience, and mental disorders. She received her Ph.D. in computer engineering from the University of California, Santa Cruz in 2009. She was a post-doctoral researcher in the Computation & Neural Systems, and Division of Biology at the California Institute of Technology from 2009 to 2011.

Prior to joining the University of Minnesota, Qi was an assistant professor in the Department of Electrical and Computer Engineering and the Department of Ophthalmology at the National University of Singapore. She has published more than 50 journal and conference papers in top computer vision, machine learning, and cognitive neuroscience venues, and edited a book with Springer, titled *Computational and Cognitive Neuroscience of Vision*, that provides a systematic and comprehensive overview of vision from various perspectives, ranging from neuroscience to cognition, and from computational principles to engineering developments. She is a member of the IEEE since 2004.